

The theory of diffraction-limited resolution in microparticle image velocimetry

Carl D Meinhart¹ and Steven T Wereley²

¹ Department of Mechanical and Environmental Engineering, University of California, Santa Barbara, CA 93106, USA

² School of Mechanical Engineering, Purdue University, 585 Purdue Mall, West Lafayette, IN 47907, USA

Received 5 December 2002, in final form 28 April 2003, accepted for publication 6 May 2003

Published 17 June 2003

Online at stacks.iop.org/MST/14/1047

Abstract

A theory of diffraction-limited spot size is developed for infinity-corrected microscope optics. Previously reported formulae were originally derived using a single-lens system. In addition, the previously reported relationship between f -number and numerical aperture assumed a paraxial approximation and was limited to air-immersion lenses. Here, a new relationship between f -number and numerical aperture is developed, and is valid for all numerical apertures and all immersion media. In addition, a new theory is developed that estimates the effective numerical aperture of an oil-immersion lens when imaging into fluid of a lower refractive index, such as water. The results indicated that when imaging into water, high numerical aperture $NA = 1.0$ or 1.2 water-immersion lenses provide comparable and sometimes better diffraction-limited resolution than $NA = 1.4$ oil-immersion lenses. In addition, when imaging into water, water-immersion lenses may provide superior image quality, because they are corrected for aberrations resulting from the water/glass interface.

Keywords: micron resolution particle image velocimetry, spatial resolution

(Some figures in this article are in colour only in the electronic version)

1. Introduction

Since the introduction of micro-PIV (particle image velocimetry) by Santiago *et al* (1998), micro-PIV has become an important diagnostic tool for microelectromechanical systems (MEMS)-based microfluidic devices. Micro-PIV differs from traditional macroscopic PIV in a variety of aspects, including the illumination and recording optics, the flow-tracing particles and the image-processing algorithms. Typically in micro-PIV, a volume of light is used to broadly illuminate fluorescently labelled submicron particles. In traditional PIV, a sheet of light is used to illuminate only the in-focus plane of particles. The image recording optics in micro-PIV are typically some form of microscope optics, which are characterized by high magnification and large apertures. The large apertures are used to increase the

diffraction-limited resolution of the system. The resolution of micro-PIV is limited ultimately by the diffraction limits of the recording optics. Therefore, it is important to have a solid working theory of the diffraction limits of microscope optics.

Adrian and Yao (1985) developed a theory to describe the diffraction-limited resolution of PIV. Their theory is widely used for standard PIV techniques, where a single-lens system is used to image through an air medium into a gaseous or aqueous fluid. Microscopic recording systems consist of at least two lens assemblies, an objective lens and a relay lens. Furthermore, the objective lens may be designed to image through a high-refractive-index fluid, such as water or oil, to improve the numerical aperture of the lens.

The microscope literature deals with diffraction-limited spot size indirectly. Microscopists are interested primarily in the resolving power of the lens. The resolving power is

the minimum transverse distance by which two objects can be separated while still being resolved using the Rayleigh criterion (Inoue and Spring 1997).

Santiago *et al* (1998) and Meinhart *et al* (1999) present two different formulae describing the diffraction-limited spot size for micro-PIV. As will be shown in this paper, both of these equations have shortcomings. The equation presented by Santiago *et al* (1998) assumes a single-lens system. Both formulae (Santiago *et al* 1998, Meinhart *et al* 1999) assume the imaging medium is air, and assume the paraxial approximation to relate f -number to numerical aperture. Even though these two approximations are not valid, the resulting formulae provide an order of magnitude estimation of the diffraction-limited spot size.

Olsen and Adrian (2000) present a theory that estimates the out-of-plane measurement thickness. Their results indicate that the thickness of the measurement plane depends strongly on f -number. Since most objective lenses used for micro-PIV are specified by numerical aperture instead of f -number, it is important to understand the relationship between these two parameters. Here we present a theory that relates numerical aperture and f -number for infinity-corrected lenses.

The purpose of this paper is to develop a theoretical framework explaining the diffraction limits of micro-PIV using infinity-corrected optics, which are commonly used in many modern microscopes. The theory is developed from first principles, and is compared with the formulae that have appeared previously in the literature. Some microscopes exist that do not incorporate infinity-corrected optics. In these situations, the theory presented here may be used with caution to approximate roughly their diffraction-limited performance.

2. Diffraction-limited spot size

2.1. Fraunhofer diffraction

The electromagnetic disturbance of monochromatic light due to diffraction through a well-corrected lens can be expressed in terms of the Fraunhofer diffraction formula (Born and Wolf 1997)

$$U(P) = C \iint_A e^{-ik(p\xi+q\eta)} d\xi d\eta \quad (1)$$

where $U(P)$ is the disturbance, k is the wavenumber, (p, q) are the directional cosines of point P , A denotes that the area integral is over the lens aperture, and C is a constant. The electromagnetic distribution can be related to the intensity distribution by

$$I = |U|^2. \quad (2)$$

In the case of a circular aperture, it is convenient to use polar coordinates (ρ, θ) to describe a point in the aperture, such that

$$\begin{aligned} \rho \cos \theta &= \xi \\ \rho \sin \theta &= \eta. \end{aligned} \quad (3)$$

(ω, ψ) are polar coordinates of the directional cosines (p, q) , for locating point P in the image plane, such that

$$\begin{aligned} \omega \cos \psi &= p \\ \omega \sin \psi &= q. \end{aligned} \quad (4)$$

Integrating over a circular aperture of radius $D_a/2$, equation (1) becomes

$$U(P) = C \int_0^{D_a/2} \int_0^{2\pi} e^{-ik\rho\omega\cos(\theta-\psi)} \rho d\rho d\theta. \quad (5)$$

Following Born and Wolf (1997), integration of equation (5) yields

$$U(P) = C \frac{\pi D_a^2}{4} \left(\frac{2J_1(s)}{s} \right), \quad (6)$$

and the intensity distribution

$$I(P) = |U(P)|^2 = \left(\frac{2J_1(s)}{s} \right)^2 I_0. \quad (7)$$

where I_0 is the peak intensity, J_1 is a first-order Bessel function of the first kind and $s = k\omega D_a/2 = \pi\omega D_a/\lambda$. The first zero in J_1 occurs at a value $s_0 = 1.22\pi$. The first dark ring occurs at

$$s_0 = 1.22\pi = \pi\omega_0 D_a/\lambda. \quad (8)$$

The diameter of the point spread function, d_s , is defined by the diameter of the first dark ring in the image plane. Writing the directional cosine of the first dark ring in terms of the image distance, s_i , such that $\omega_0 = d_s/2s_i$, yields the well known result for the diameter of the point spread function

$$d_s = \frac{2.44s_i\lambda}{D_a}. \quad (9)$$

2.2. Single-lens system

Figure 1 shows a schematic of a single thin lens, with aperture diameter, D_a . Assuming the paraxial approximation, the width of the point-spread function is given by equation (9). Combining the Gaussian lens formula and an expression for magnification

$$\begin{aligned} \frac{1}{s_i} + \frac{1}{s_o} &= \frac{1}{f} \\ M &= \frac{s_i}{s_o}, \end{aligned} \quad (10)$$

yields

$$s_i = (M + 1)f, \quad (11)$$

where M is magnification and f is the focal length of the lens. Combining equations (9) and (11) and using the definition of f -number, $f^\# \equiv f/D_a$, one obtains the well known expression for diffraction-limited spot size through a single lens (see Adrian and Yao 1985, Adrian 1991)

$$d_{s_p} = 2.44(M + 1)\lambda f^\#. \quad (12)$$

Equation (12) is well suited for describing the diffraction-limited spot size in macroscopic PIV systems, because they often use single photographic-type lenses where f -number is commonly used to describe their speed. We use the term d_{s_p} to denote the diffraction-limited spot size of a photographic lens.

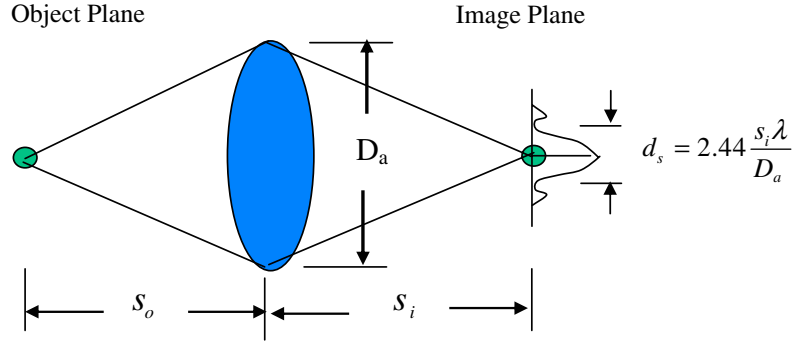


Figure 1. Schematic of a single thin lens with aperture diameter, D_a . The point spread function through a circular aperture is the well-known Airy function of width, $d_s = 2.44s_i\lambda/D_a$.

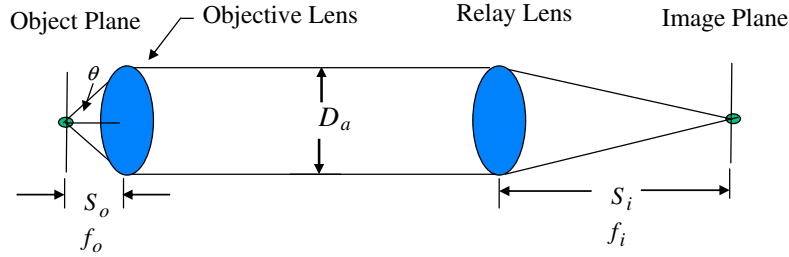


Figure 2. Schematic of an infinity-corrected optical system. The system consists of an objective lens and a relay lens. For high magnification, the focal length of the relay lens is much larger than the focal length of the objective lens.

2.3. Infinity-corrected optics

In micro-PIV, it is common to use an infinity-corrected optical system to record submicron particles with relatively high magnification (Santiago *et al* 1998, Meinhart *et al* 1999). Figure 2 shows an idealization of an infinity-corrected system. In this system, the object plane is located at the focal length of the objective lens, such that a point source of light is refracted into parallel light rays. One advantage of the system is that the distance between the objective lens and the relay lens can be changed without affecting the magnification. In addition, optical filters and mirrors can be inserted between the lenses without distorting the image.

The object distance and the image distance are set equal to the focal length of the objective lens and the relay lens respectively. Therefore, the magnification can be written in terms of the focal lengths

$$M \equiv \frac{s_i}{s_o} = \frac{f_i}{f_o}. \quad (13)$$

Defining the f -number of the objective lens

$$f_\infty^\# \equiv \frac{f_o}{D_a}. \quad (14)$$

Combining equations (9), (13) and (14), one obtains the expression for the diffraction-limited spot size produced by infinity-corrected optics, d_{s_∞}

$$d_{s_\infty} = 2.44M\lambda f_\infty^\#. \quad (15)$$

In the limit of large magnification, the formulae given by equations (12) and (15) become similar. From an academic viewpoint, it is important to understand the origins of these two

expressions, and under which conditions they are applicable. We suggest using equation (15) for infinity-corrected optical systems.

3. Relationship between $f^\#$ and NA

The speed of a photographic lens is commonly described by its f -number, $f^\#$. The light-gathering power of a microscope lens can be measured by the square of its numerical aperture, NA. Most microscope lenses are classified by NA; however, the diffraction-limited spot size given by equation (15) is written in terms of $f_\infty^\#$. Therefore, it is necessary to determine the relationship between $f_\infty^\#$ and NA.

The numerical aperture of a microscope lens is defined as

$$NA = n_o \sin \theta, \quad (16)$$

where n_o is the refractive index of the immersion medium between the object and objective lens, θ is the half-angle of the cone of light subtended by the objective lens (see figure 2 and Hecht 1989). For infinity-corrected lenses

$$f_\infty^\# \equiv \frac{f_o}{D_a} = \frac{s_i}{D_a} = \frac{1}{2 \tan \theta}. \quad (17)$$

Combining the trigonometry identity

$$\tan \theta = \left(\frac{1}{\sin^2 \theta} - 1 \right)^{-1/2}, \quad (18)$$

with equations (16) and (17) yields

$$f_\infty^\# = \frac{1}{2} [(\sin \theta)^{-2} - 1]^{1/2} = \frac{1}{2} \left[\left(\frac{n_o}{NA} \right)^2 - 1 \right]^{1/2}. \quad (19)$$

Table 1. Characteristic values of f -number and diffraction spot size for various microscope lenses.

M	n_o	NA	$f_p^\#$	$f_\infty^\#$	d_{sp} (μm)	$d_{s\infty}$ (μm)
10	1.000	0.25	2.00	1.90	33.3	29.3
20	1.000	0.50	1.00	0.87	31.8	26.2
40	1.000	0.60	0.83	0.67	51.7	40.3
40	1.000	0.75	0.67	0.44	41.4	26.7
60	1.330	1.00	0.50	0.44	46.1	39.8
60	1.330	1.20	0.42	0.24	38.4	21.7
60	1.515	1.40	0.36	0.21	33.0	18.8

Photographic systems incorporated in macroscopic PIV typically image through air (i.e. $n_o = 1$), and have relatively large $f^\#$ compared with microscope objective lenses. The large $f^\#$ implies the paraxial approximation $\theta \ll 1$ and $\text{NA} = \sin \theta \sim \tan \theta \sim \theta$. Applying these assumptions reduces equation (19) to the paraxial approximation for air-immersion lenses, $f_p^\#$, reported previously in the micro-PIV literature by Santiago *et al* (1998) and implicitly used by Olsen and Adrian (2000)

$$f_p^\# = \frac{1}{2\text{NA}}. \quad (20)$$

In summary, there are two formulae for diffraction-limited spot size. For an air-immersion single-lens system subject to the paraxial approximation, the diffraction-limited spot size is given by

$$d_{sp} = 1.22(M + 1)\lambda/\text{NA}. \quad (21)$$

Equation (21) has been used throughout the micro-PIV literature, and provides a reasonable estimate of d_s , but may not be as precise as that for an infinity-corrected system

$$d_{s\infty} = 1.22M\lambda[(\sin \theta)^{-2} - 1]^{1/2} = 1.22M\lambda \left[\left(\frac{n_o}{\text{NA}} \right)^2 - 1 \right]^{1/2}. \quad (22)$$

It is clear from equation (22) that the half-angle subtended by the lens, θ , determines the diffraction-limited spot size, and not the numerical aperture directly. Therefore, it may be sufficient to use lower numerical aperture lenses, such as air- or water-immersion lenses instead of oil-immersion lenses, provided θ remains sufficiently large.

Table 1 compares values of $f_p^\#$, $f_\infty^\#$, d_{sp} and $d_{s\infty}$ for various microscope lenses. As expected, the paraxial approximation for f -number, $f_p^\#$, agrees with $f_\infty^\#$ for the $M = 10$, $\text{NA} = 0.25$ lens. However, for higher-NA lenses, the approximation is not accurate. The difference between d_{sp} and $d_{s\infty}$ is significant for all lenses, with larger differences occurring for higher-NA lenses.

One of the major results of equation (22) is that $d_{s\infty}$ only depends upon the half-angle subtended by the lens, and not directly upon the numerical aperture and lens immersion medium. Therefore, similar diffraction-limited spot sizes can be achieved with an $M = 60$ $\text{NA} = 1.2$ water-immersion lens, $d_{s\infty} = 21.7 \mu\text{m}$, compared with an $M = 60$ $\text{NA} = 1.4$ oil-immersion lens, $d_{s\infty} = 18.8 \mu\text{m}$. Therefore, in micro-PIV experiments requiring high spatial resolution, it may be advantageous to use water-immersion lenses, even though they may have lower numerical apertures than oil-immersion lenses.

4. Resolving power of a lens

It is clear from equations (15) and (22) that $f_\infty^\#$ is a more direct parameter for determining diffraction-limited spot size than NA. In order to understand the importance of NA, one must understand the difference between diffraction-limited spot size and resolving power. Microscope lenses are designed to image microscale objects with relatively large magnification (i.e. $M \sim 10$ – 100). The resolution limits of imaging with an optical microscope are best described by the resolving power, instead of the diffraction-limited spot size. In contrast, the spatial resolution of micro-PIV systems is ultimately limited by the diffraction-limited spot size of the imaging system. Ernst Abbe (1840–1905) originally introduced the concept of numerical aperture to describe the resolving power of a microscope lens (Hecht 1989). The resolving power of a lens is defined as the minimum transverse distance between two point sources of light, r , that can be resolved using the Rayleigh criterion (Jenkins and White 1957, Cosslett 1966, Hecht 1989).

Upon inspection of figure 3(a), the location of the of the first minimum of the Airy function, $r' = d_s/2 = 1.22s_i\lambda/D_a$, can be written in terms of the critical angle, α_{cr}

$$\begin{aligned} \frac{r'}{s_i} &= 1.22 \frac{\lambda}{D_a} \\ \frac{r'}{s_i} &= \tan \alpha_{cr} \approx \alpha_{cr}, \end{aligned} \quad (23)$$

such that

$$\alpha_{cr} \approx 1.22 \frac{\lambda}{D_a}. \quad (24)$$

The path difference between points A and B to the first minimum can be expressed as $\delta_{cr} = D_a \sin \alpha_{cr} \approx D_a \alpha_{cr}$, such that

$$\delta_{cr} \approx 1.22\lambda. \quad (25)$$

Following similar arguments by Jenkins and White (1957), figure 3(b) depicts the path difference between two points O and O' , separated by a distance r , to point A , as $\delta_1 = n_o r \sin \theta$. The refractive index, n_o , corrects for immersion media with optical densities greater than that of air. For self-luminous objects, such as fluorescent particles, one must also take into account that path difference between O and O' to point B , such that $\delta_2 = n_o r \sin \theta$ (see figure 3(c)). Equating $\delta_{cr} = \delta_1 + \delta_2$, using equations (16) and (25), and solving for r , yields the resolving power of a microscope lens for self-luminous objects (Jenkins and White 1957)

$$r = \frac{1.22\lambda}{2\text{NA}}. \quad (26)$$

The resolving power given by equation (26) looks remarkably similar to the paraxial approximation for diffraction-limited spot size, equation (21), but is derived in a very different manner. The definition of numerical aperture, $\text{NA} = n_o \sin \theta$, is remarkably similar to Snell's law; however, this is coincidental.

5. Effective numerical aperture

In experiments where the highest possible spatial resolution is desired, researchers may use high-numerical-aperture

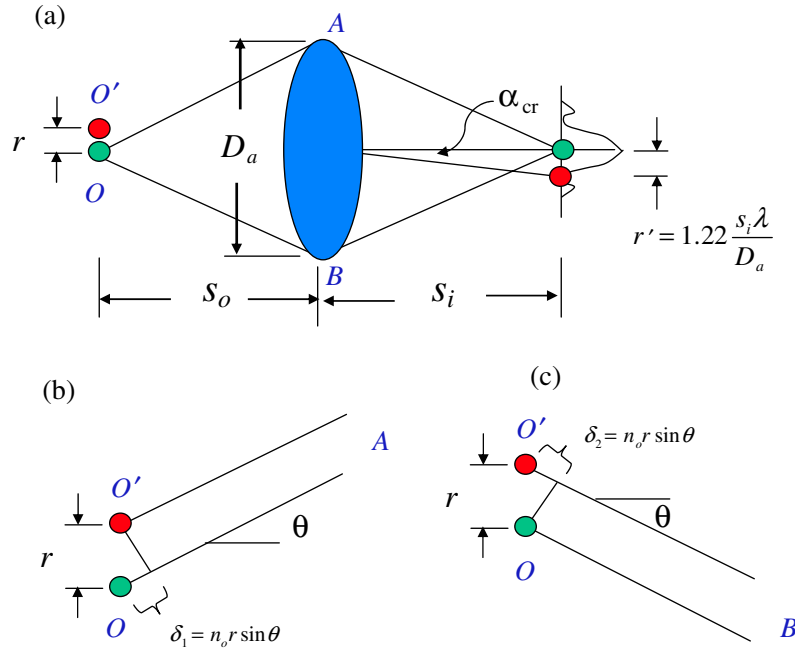


Figure 3. Geometry illustrating the resolving power of a single lens, which is defined as the minimum separation distance, r , of two point sources of light. The critical angle, α_{cr} , is determined from the Rayleigh resolution criterion.

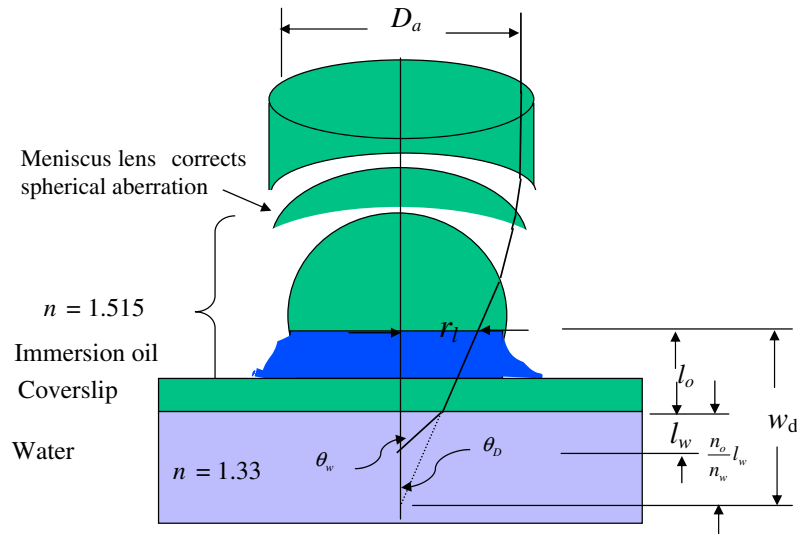


Figure 4. Geometry of a high numerical aperture oil-immersion lens, immersion oil, coverslip, and water as the working fluid. A point source of light emanating from a depth in the water, l_w , appears to be at a distance w_d from the lens' entrance.

oil-immersion lenses (e.g. Santiago *et al* 1998, Meinhart *et al* 1999). When the index of refraction of the working fluid is lower than the immersion medium, the effective numerical aperture is lower than the design numerical aperture. In this section, a theory is presented that estimates the effective numerical aperture.

For the purpose of specificity, assume an oil-immersion lens is used to image into water through a coverslip with an index of refraction matching that of the oil. This is a very common situation in micro-PIV. This analysis is easily generalizable to other arrangements, such as using an oil-immersion lens to image a gas flow—or generally from any arbitrary immersion medium into any working fluid. From figure 4, the distance from the objective lens to the water/glass

interface is l_o , and the imaging distance into the water is l_w . Since the refractive index of water, n_w , is less than the refractive index of oil and glass, n_o , to within the paraxial approximation, the object plane appears to be a distance $n_o l_w / n_w$ into the water. For high-numerical-aperture lenses, the paraxial approximation is not strictly valid for marginal rays, but it will give a reasonable first-order approximation.

Defining the working distance of the lens, w_d , as the distance between the edge of the lens and the apparent object plane, the paraxial approximation yields

$$w_d = \frac{n_o}{n_w} l_w + l_o. \quad (27)$$

The aperture stop can be located anywhere in the objective lens. However, as a first approximation, we can assume the

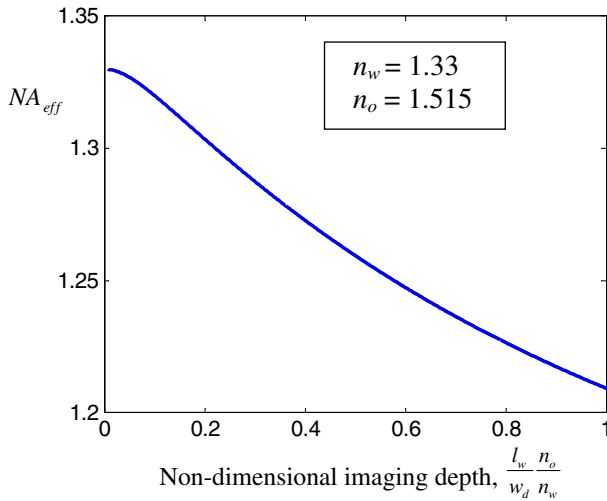


Figure 5. Effective numerical aperture of an oil-immersion lens imaging into water. The effective numerical aperture is a function of the imaging depth into the water. At the water surface, the effective numerical aperture is $NA_{eff} \approx 1.33$. At the maximum imaging depth, the effective numerical aperture is reduced to $NA_{eff} \approx 1.21$.

rim of the lens is the effective aperture stop, which defines the marginal ray. From geometry the radius of the rim is expressed as

$$\begin{aligned} r_l &= l_w \tan \theta_w + l_o \tan \theta_o \\ r_l &= w_d \tan \theta_D, \end{aligned} \quad (28)$$

where θ_D is the maximum design angle of the lens, which is fixed by the manufacturer, θ_w and θ_o are the angles of incidence of a marginal ray in the water and oil medium respectively. The angles θ_w and θ_o vary with l_w

$$w_d \tan \theta_D = l_w \tan \theta_w + \left(w_d - \frac{n_o l_w}{n_w} \right) \tan \theta_o. \quad (29)$$

Using equation (29), the identity given by equation (18), Snell's law, $n_o \sin \theta_o = n_w \sin \theta_w$, and simplifying yields an implicit equation for effective numerical aperture, $NA_{eff} = n_o \sin \theta_o$, in terms of the design numerical aperture, $NA_D \equiv n_o \sin \theta_D$, the lens's working distance, w_d , and the imaging depth in the water, l_w

$$\frac{w_d}{\left[\left(\frac{n_o}{NA_D} \right)^2 - 1 \right]^{1/2}} = \frac{l_w}{\left[\left(\frac{n_w}{NA_{eff}} \right)^2 - 1 \right]^{1/2}} + \frac{w_d - \frac{n_o l_w}{n_w}}{\left[\left(\frac{n_o}{NA_{eff}} \right)^2 - 1 \right]^{1/2}}. \quad (30)$$

It is convenient to solve numerically for imaging depth, l_w , in terms of NA_{eff} . Figure 5 shows the solution of equation (30) using $n_o = 1.515$ and $n_w = 1.33$. When imaging at the coverslip/water surface, $l_w = 0$, the effective numerical aperture is approximately equal to the refractive index of the water, $NA_{eff} \approx 1.33$. The effective numerical aperture decreases with increasing imaging depth. At the maximum imaging depth, $l_w = n_w w_d / n_o$, the effective numerical aperture is reduced to approximately $NA_{eff} \approx 1.21$ (see table 2).

The change in refractive index at the water/glass interface significantly reduces the effective numerical aperture of the lens, which increases the diffraction-limited spot size.

Table 2. Estimates of the diffraction-limited spot size, $d_{s\infty}$, for various effective numerical apertures, NA_{eff} .

NA_{eff}	$d_{s\infty}$ (μm)	Imaging medium	Imaging depth
1.4	18.8	Oil	N/A
1.33	24.8	Water	Minimum
1.21	34.2	Water	Maximum

Table 2 shows how the diffraction-limited spot size, $d_{s\infty}$, varies with NA_{eff} , for $M = 60$, $NA_D = 1.4$, $\lambda = 0.62 \mu\text{m}$.

In experiments where the working fluid is water, similar diffraction-limited spot sizes can be achieved using an $NA = 1.0$ water-immersion lens, $d_{s\infty} = 39.8 \mu\text{m}$, compared to an $NA_D = 1.4$ oil-immersion lens, which may only achieve an effective numerical aperture of $NA_{eff} \approx 1.21$, where $d_{s\infty} = 34.2 \mu\text{m}$. Superior performance will be achieved by an $NA = 1.2$ water-immersion lens, where $d_{s\infty} = 21.7 \mu\text{m}$. Further, since the water-immersion lens is designed to image into water either with or without a coverslip, the image quality will be superior to the oil-immersion lens.

6. Conclusions

A new theory is developed to describe the diffraction-limited spot size of infinity-corrected microscope optics, $d_{s\infty}$. The theory shows that $d_{s\infty}$ depends upon the maximum angle subtended by the lens and not directly upon the numerical aperture and the refractive index of the immersion medium. This is in direct contrast to the resolving power of a microscope lens. Consequently, an $NA = 1.2$ water-immersion lens will have comparable diffraction resolution to an $NA = 1.4$ oil-immersion lens. In addition, the diffraction-limited spot size theory for infinity-corrected optics predicts smaller spots than those predicted by the more commonly used single-lens, paraxial approximation, d_{sp} .

Several researchers have used oil-immersion objective lenses to image into water. A theory is developed to estimate the effective numerical aperture, NA_{eff} , resulting from the refractive index of the water being lower than the refractive index of the immersion oil. For an oil-immersion lens with a design numerical aperture $NA_D = 1.4$, the effective numerical aperture is $NA_{eff} \approx 1.33$ when imaging near the water/glass interface and $NA_{eff} \approx 1.21$ when imaging deep into the water. With this reduction in effective numerical aperture, similar diffraction resolutions can be achieved using an $NA = 1.0$ water-immersion lens. In addition, when imaging into water, water-immersion lenses will have less geometric distortion than oil-immersion lenses. This suggests that when spatial resolution of the order of $1 \mu\text{m}$ is required, $NA = 1.0$ water-immersion lenses may produce comparable or even higher-resolution results than the more commonly used $NA = 1.4$ oil-immersion lens.

Acknowledgments

The authors would like to thank Professor Ronald J Adrian from the University of Illinois for his many discussions and insight into imaging theory. This work is supported by DARPA/ARMY DAAD 19-00-1-0400, DARPA/Air Force F30602-00-2-0609, NSF CTS-9874839 and NSF ACI-0086061.

References

- Adrian R J 1991 Particle-imaging techniques for experimental fluid mechanics *Annu. Rev. Fluid Mech.* **23** 261–304
- Adrian R J and Yao C S 1985 Pulsed laser technique application to liquid and gaseous flows and the scattering power of seed materials *Appl. Opt.* **24** 44–52
- Born M and Wolf E 1997 *Principles of Optics* (Oxford: Pergamon)
- Cosslett V E 1966 *Modern Microscopy* (Ithaca, NY: Cornell University Press)
- Hecht E 1989 *Optics* 2nd edn (Reading, MA: Addison-Wesley)
- Inoue S and Spring K 1997 *Video Microscopy: The Fundamentals* (New York: Plenum)
- Jenkins F A and White H E 1957 *Fundamentals of Optics* 3rd edn (New York: McGraw-Hill)
- Meinhart C D, Wereley S T and Santiago J G 1999 PIV measurements of a microchannel flow *Exp. Fluids* **27** 414–19
- Olsen M G and Adrian R J 2000 Out-of-focus effects on particle image visibility and correlation in microscopic particle image velocimetry *Exp. Fluids (Suppl.)* S166–S174
- Santiago J G, Wereley S T, Meinhart C D, Beebe D J and Adrian R J 1998 A PIV system for microfluidics *Exp. Fluids* **25** 316–19